

Spectral Shift in Retinal Chromophore of bacteriorhodopsin (bR) Protein in Different Medium

¹ Satish Kumar, ² Ashok Jangid

¹ Assistant Professor,

¹ Department of Physics & Computer Science

¹ Daylabh Educational Institute, Dayalbagh, Agra-05, India

² Associate Professor

² Department of Physics & Computer Science

² Daylabh Educational Institute, Dayalbagh, Agra-05, India

Abstract: Bacteriorhodopsin (bR) is light sensitive protein in purple membrane of halobacterium salinarum. Chromophore is region in the bR molecule corresponding to visible and ultraviolet spectrum. Chromophore of bR has been investigated using quantum mechanical approach. Spectral shift in absorption was found in water medium as comparison to gases medium. A retinal chromophore is attached with lysine amino acid of one α helix of proteins structure. Absorption spectra and circular dichroism spectra of retinal chromophore with lysine opsin has been calculated. Energies of the seven electronically excited states of chromophore has been calculated for all nonbonding orbitals n , and bonding and anti bonding π and π^* molecular orbitals (MOs). The complete active space self consisting field CASSCF and N-electrons valence perturbation theory of second order NEVPT2 methods are applied to calculate energies of electronically excited states. In CASSCF, calculation 10 active electrons were kept in 9 active orbitals. All energies of electronically excited were calculated around the HOMO and LUMO orbitals as these being most probable transitions for the active electrons. Time dependent density functional theory TD-DFT method has been applied to calculate the absorption spectra and CD spectra. CD spectra is selective absorption of one of the two orthogonal component of two linearly plane polarized incident light beams. Study shows that an isotropic nature of medium causes strong asymmetric or preferential absorptions of one field component and transparent for second orthogonal component.

Keywords- Bacteriorhodopsin-bR, Protonated Schiff base- PSB, Complete active self consist field theory- CASSCF, N-electrons valence perturbation theory to second order-NEVPT2, Time dependent density functional theory- TD-DFT and Circular dichroism-CD

I. INTRODUCTION

Rhodopsins are retinal proteins which are very important to understand the various processes viz. in vision, bioenergetics and phototaxis [1, 2]. The retinal chromophore plays a crucial role in absorption of light in proteins by protonated schiff base linkage (PSB) to the apoprotein which triggers the response of protein to light. The environment of protein regulates the absorption of retinal chromophore. The maximum absorption drastically changes in presence of apoprotein and this effect is known as the opsin shift [3]. The absorption spectrum have wide range from 360 to 635 nm [4]. It is a challenge in vision research that how maximum absorption is adjusted in retinal chromophore for the wide range of wavelength. Spectral tuning in retinal chromophore was observed in methanol environment recently which gives a new idea to design retinal based photo active molecular devices and it has been invented an interdisciplinary area of research named as bioelectronics [5, 6].

The cone cell pigments of human retina absorb blue light (425 nm), green (530 nm) and red (560 nm) which provide the solid basis for a sense of color [7]. Now a day's availability of crystallographic structure of light driving bacteriorhodopsin makes it possible to understand the spectral tuning [8-10]. The diversity of the absorption spectra has been studied and several explanations have been given [11-15]. The maximum wavelength absorption of retinal is adjusted by replacing amino acids in the retinal binding pocket. The genetics of color blindness and proteorhodopsin are important sources of information for vision process [16-18]. Understanding the color vision in biological species is of fundamental importance. The cellular membrane of Halobacteria consist four type of photoactive rhodopsins viz. bacteriorhodopsin (bR), halorhodopsin (hR), sensory rhodopsin (sRI) and sensory rhodopsin (sRII) [19-21]. In bacteriorhodopsin (bR) of Halobacterium salinarum, incident light energy is absorbed by retinal chromophore and, is used through initial all-trans to 13-cis photo isomerization reaction of retinal chromophore which establishes an electrochemical gradient across the membrane. The spectral change in rhodopsin is based on the response of retinal chromophore to external stress and the polarization of amino acids of the protein environment.

The dipole moment of an excited state of the chromophore is changed because of high electronic polarisability and structural flexibility. The PSB of retinal has changed the dipole moment by 12 D (Cl^-) when it is excited into higher states [22]. It can be achieved by using the polarizable force field or implicit solvent model [23-28] of lysine amino acid via PSB linkage. On absorption of light, the charge distribution of electronic excited states is changed. The positive charge is located around the PSB linkage but after absorptions it shift towards β -ionone ring of retinal [23]. The shorter the distance between the PSB linkage group and negative charged groups of counterion such as Asp85 and Asp212 in bR will lead to a blue shift spectrum [11, 29] [16]. The counterion effect has been verified by decreasing the pH of the protonation of the anionic residue [18]. The engineering of

proteins acquires chromophore which exhibit desired colorimetric, fluorescent and photo chromic properties. It is revolutionizing idea which gives control over the observation of cellular states [30-37]. The rhodopsins are used to developing optical probes which absorbed the wide range of colors and have exhibited the photo chromic behavior for channelrhodopsin [38, 39] and octopus rhodopsin [40] ASR and different mutant of bacteriorhodopsin [41, 42]. In the same way, Cohen and co-workers have recently reported for two rhodopsin-based voltage-sensitive fluorescent proteins i.e. proteorhodopsin optical proton sensor and archaerhodopsin3 [43, 44].

In bacteriorhodopsin, the chromophore is the region where light interact with the molecules and responsible for its colors. So it is interesting to understand the absorption and emission spectra of bacteriorhodopsin with quantum mechanical methods such as CAPST2/CASSCF and TD-DFFT. NEVPT2/CASSCF and MP2 methods are based on quantum principles, include the effects of electronic dynamical correlation such as multiconfigurational interaction or multi reference second order perturbation theory. The results of NEVPT2/CASSCF calculations are similar to CAPST2/ CASSCF results. Both methods are used to calculate the energy of the excited states of chemical or biological systems. CAPST2 calculation gives satisfactory results of relative energy between the different electronic states [45]. The photoisomerization process and photostability have been studied by CAPST2/CASSCF and TDDFT/CASSCF successfully [46]. TD-DFT method are applied to calculate the UV-Vis absorption spectra, for large transition of metal complexes of excited states in solution in terms of band separation [47] .

II. BRIEF DESCRIPTION OF CASSCF/NEVPT2 METHOD

CASSCF/NEVPT2 method is an ab initio self-consistent field method, used to calculate the energies of the excited states of a molecule. It is an extended form of Hartree Fock method and its wave function of electronic state can be written as

$$|\psi_z^s\rangle_{\text{CASSCF}} = \sum \chi C_{\chi L} |\phi_{\chi}^s\rangle \quad (1)$$

Where, $|\psi_z^s\rangle_{\text{CASSCF}}$ is N-electron CASSCF wave functions for the state Z and with spin S and $|\phi_{\chi}^s\rangle$ is the set of all configurational states (CSF) in the form of Slater determinant. $C_{\chi L}$ is coefficient of variational parameters. The CSF is set of orthonormal wave functions of molecular orbitals $\psi_i(r)$ which are expanded form of the basis functions

$$\psi_i(r) = \sum_q C_{qi} \phi_q(r) \quad (2)$$

Where, C_{qi} molecular orbits (MO) constant from the 2nd set of variational parameter. Once the CASSCF wave functions are known then, the energy of selected states is calculated by Rayleigh quotient method. The expression for energy is given in equation (2.3)

$$E = \frac{\langle \psi_i^s | \hat{H} | \psi_i^s \rangle}{\langle \psi_i^s | \psi_i^s \rangle} \quad (3)$$

In NEVPT2 theory, the first-order wave function is spanned by vectors that are obtained from the contracted single and double excitation operators acting on the reference wave function. To understand the application of the NEVPT2 method on calculated CASSCF wave functions. Consider the zeroth order wave functions ψ^0 function corresponding to the zeroth order E^0 energy which is a complete solution of complete active space configuration interaction that is obtained by the CASSCF method. The Hamiltonian of the system is divided into three parts (i) core of orbitals, (ii) active part of orbitals, and (iii) virtual parts of the orbitals. The core or inner orbitals are represented by i, j, k..., active orbitals labeled as a, b, c...and virtual orbitals labeled as r, s, t....The Dyall Hamiltonian consist Fock type operators in the core and virtual spaces, and Hamiltonian in the active space [48]. The expression of the Hamiltonian is written as

$$H^D = F_{\text{core}} + H_{\text{act}} + F_{\text{ext}} \quad (4)$$

$$F_{\text{core}} = \sum_i \varepsilon_i a_i^* a_i + C \quad (5)$$

$$H_{\text{act}} = \sum_{ab \in \text{act}} h_{ab}^{\text{eff}} a_a^* a_b + \sum_{abcd \in \text{act}} v_{abcd} a_a^* a_b^* a_c a_d \quad (6)$$

$$F_{\text{ext}} = \sum_r \varepsilon_r a_r^* a_r \quad (7)$$

$$H^D \psi^0 = E^0 \psi^0 \quad (8)$$

It is to be noted that H_{act} includes the Coulombic field with core electrons. C is a constant for expectation value of Dyall Hamiltonian with zero order wave function. The body integrals in MOs basis are denoted by v_{abcd} . The first order wave function is expanded in restricted perturbed functions and these perturbed function can be written in eight subspaces contracted to set of determinants and contracted coefficient are defined from the perturbation theory. First, B is divided in eight components that connect the reference wave function and eight spaces. It can be written as

$$B = \sum_{i<j,r<s} B_{ijrs}^0 + \sum_{i<j,r} B_{ijr}^{+1} + \sum_{r<s,i} B_{rsi}^{-1} + \sum_{i<j} B_{ij}^{+2} + \sum_{r<s} B_{rs}^{-2} + \sum_i B_i^{+1'} + \sum_r B_r^{-1'} + \sum_{ir} B_{ir}^{0'} \quad (9)$$

$$B_{ijrs}^0 = \langle rs || ji \rangle a_{ij}^{rs} \quad (10)$$

$$B_{ijr}^{+1} = \sum_a \langle ra || ji \rangle a_{ij}^{ra} \quad (11)$$

$$B_{rsi}^{-1} = \sum_a \langle rs || ia \rangle a_{ai}^{rs} \quad (12)$$

$$B_{ij}^{+2} = \sum_{a<b} \langle ab || ji \rangle a_{ij}^{ab} \quad (13)$$

$$B_{rs}^{-2} = \sum_{a<b} \langle rs || ba \rangle a_{ab}^{rs} \quad (14)$$

$$B_i^{+1'} = \sum_{a<b,c} \langle ab || ic \rangle a_{ci}^{ab} + \sum_{aj} \langle aj || ij \rangle a_{ji}^{aj} + \sum_a \langle a | h | i \rangle a_i^a \quad (15)$$

$$B_r^{-1'} = \sum_{a,b<c} \langle ra || cb \rangle a_{bc}^{ra} + \sum_{aj} \langle rj || aj \rangle a_{ja}^{rj} + \sum_a \langle a | h | r \rangle a_a^r \quad (16)$$

$$B_{ir}^{0'} = \sum_{ab} \langle ra || ib \rangle a_{bi}^{ra} + \sum_j \langle rj || aj \rangle a_{ja}^{rj} + \langle r | h | i \rangle a_a^r \quad (17)$$

The perturbed function are obtained by applying each of the component perturbations to zeroth order wave functions in normalized form and these expression are written as follows till all the wave function is not calculated.

$$\Omega_{ijrs}^0 = \frac{1}{\sqrt{N_{ijrs}^0}} B_{ijrs}^0 \psi^0 \quad (18)$$

$$\Omega_{ijr}^{+1} = \frac{1}{\sqrt{N_{ijr}^{+1}}} B_{ijr}^{+1} \psi^0 \quad (19)$$

The every perturb function is orthogonal to the perturbed function. Now finally the perturbed function is written as

$$H^0 = A_{act} H^D A_{act} + \sum_{l,k} |\Omega_l^k \rangle E_l^k \langle \Omega_l^k| \quad (20)$$

Where $E_l^k = \langle \Omega_l^k | H^D | \Omega_l^k \rangle$, A_{act} is projection to active space. The first order perturbed wave function is in expanded form is written as

$$\psi^1 = \sum_{i<j,r<s} C_{ijrs}^0 \Omega_{ijrs}^0 + \sum_{i<j,r} C_{ijr}^{+1} \Omega_{ijr}^{+1} + \dots \quad (21)$$

The coefficient and energy contribution can be obtained using Rayleigh-Schrodinger. The coefficient $c_{ijk} = -\frac{\langle \phi_{ijk} | V | \psi \rangle}{E_{ijr} - E^0} = -\frac{\sqrt{N_{ijr}}}{E_{ijr} - E^0}$ and $E^2 = -\sum_{i,j<r} \frac{N_{ijr}}{E_{ijr} - E^0}$ where E_{ijr} is the zeroth order energy perturbation function.

III. COMPUTATIONAL DETAILS

The molecular structure coordinates of the light-driven ion pump bacteriorhodopsin is taken from the PDB data bank and based on x-ray diffraction of crystal growth on cubic lipid phase [49]. The bacteriorhodopsin of Halobacterium 1c3w is selected from the protein data bank and Halobacterium 1c3w molecules were visualized by chemera molecular modeling system [50]. First, the retinal chromophore part is selected from the bacteriorhodopsin protein.

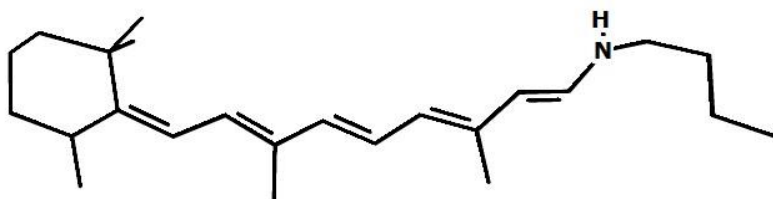


Fig.1 Schematic presentation all-trans retinal bound via PSB to Lys216 in bR.

The retinal chromophore is connected with lysine amino acid via PSB linkage. The retinal chromophore attached with lysine amino acid is shown in figure 1. Ab initio molecular orbital methods were employed to retinal chromophore for all calculations. Retinal-lysine combination was optimized with multiconfigurational, second-order Molar- Plesset perturbation theory or MP2 method by employing the 6-31G (d) basis set. The 6-31G (d) is polarizable basis function which improved the flexibility for C and N atoms of polyene back bone of retinal. The optimized structure of retinal-lysine combination is shown in figure 1. NEVPT2 /CASSCF method is inbuilt in ORCA computational tool and it is used to calculate the energy of the excited states and absorption spectra [51]. The number of active electrons and active orbitals were 10 and 9 respectively, used for CASSCF (10, 8) / NEVPT2 calculation. For quantum mechanical calculations, only retinal-lysine moiety was included. The energy of six doublets excited states was computed by ORCA.

Table1. Absorption spectrum via transition electric dipole moments in free space

States	Energy (cm ⁻¹)	λ (nm)	f_{osc}	T(au)	T _x (au)	T _y (au)	T _z (au)
S1	37784.5	264.7	0.429325949	3.74066	0.36506	1.59168	-1.03632
S2	39933.7	250.4	0.058848460	0.48514	-0.10162	-0.57397	0.38128
S3	43318.5	230.8	1.302326640	9.89743	9.89743	2.72663	-1.51279
S4	46102.4	216.9	0.440508624	3.14562	3.14562	-1.45444	1.01011
S5	47193.0	211.9	0.021167085	0.14766	-0.04326	-0.32914	0.19353
S6	50489.2	198.1	0.038345663	0.25003	0.19194	0.14877	-0.43710
S7	51844.0	192.9	0.016342844	0.10378	-0.05183	0.11914	-0.29479

Table2. Absorption spectrum via transition electric dipole moments in presence of water

States	Energy (cm ⁻¹)	λ (nm)	f_{osc}	T(au)	T _x (au)	T _y (au)	T _z (au)
S1	35896.9	278.6	0.453847489	4.16226	-0.38664	-1.67536	1.09815
S2	39583.0	252.6	0.037788783	0.31429	0.08107	0.45588	-0.31605
S3	42561.6	235.0	1.359013251	10.51190	-0.44355	-2.82437	1.52909
S4	45454.9	220.0	0.368914878	2.67190	0.07224	1.33419	-0.94161
S5	49763.1	201.0	0.043236202	0.28603	-0.21011	0.15279	-0.46749
S6	50793.5	196.9	0.046577417	0.30189	-0.33082	-0.33082	0.43804
S7	50541.1	197.9	0.001476970	0.00962	0.05227	0.05227	-0.08277

The relative energies of electronically excited states and oscillator strength for retinal-lysine amino acid are given in table 1 and table 2 in free space and water respectively. The data given in the tables are based on the TD-DFT calculation. In TD-DFT calculation the 6-31 G (d) basis function was used. The refractive index 1.33 and dielectric constant 80.8 was used for energy calculation in presence of water.

RESULTS AND DISSCUSSION

When electromagnetic energy (EM) incident to retinal chromophore of bR molecule and it absorbs the energy and, get excited to the higher states. The energy of the six excited states has been calculated by the NEVPT2 method. The spectroscopic diagram of absorption and emission is based on calculation done by using NEVPT2/CASSCF method is presented in figure 2. The energies, dipole moment, wavelength, osillator strength and transition dipole moment of all six doublet excited states are written in table 1. The charge of the excited states has changed after absorbing EM energy radiation because structural postion of an

atoms and dynamic distribution of electrons in the orbits is different from the ground state. This difference is measured in terms of change in dipole moment of different spinning electrons, in an orbitals near to highest occupied molecular orbit (HOMO) and lowest unoccupied molecular orbit (LUMO) transitions energy gap.

All the excited states have a dipole moment because of exchange of through PSB association which was different from the ground state dipole moment that is known as the transition dipole moment. The quantum mechanically, the transition dipole moment is defined as $M = \langle \psi_1 | M | \psi_2 \rangle$, where $M = \sum_i e r_j$ is known as transition moment expression. The transition rates per unit energy density of the radiation is given as $B_{12} = \frac{8\pi^3}{3h^2} |\langle \psi_1 | M | \psi_2 \rangle|^2$, where $\langle \psi_1 | M | \psi_2 \rangle = \int \psi_1 M \psi_2 dV$, and ψ_1 and ψ_2 are the wave function of the state 1 and 2 respectively. The transition dipole moment is directly related to the oscillator strength f and spectral energy density. The expression of the oscillator strength is given as $f = \frac{8\pi^2 m \nu}{3 h e^2} |\langle \psi_1 | M | \psi_2 \rangle|^2$, the dipole moment is not same for all excited states. On the basis of the above expression spectral transition between states 1 and 2 corresponding to red wavelength, the value of maximum absorption was 772.9 nm and it was observed maximum absorption 568 nm which was calculated in presence of some amino acid such as ASP (D85), ASP (D212) and some water molecules [52]. The maximum absorption was 497 nm found experimentally [53]. The absorption between S2-S1 was found 434 nm which is in good agreement to experimental data and much better than computed result in ref 47 (488 nm) and 48 (457 nm).

The value absorption data in parenthesis are the experimental data for absorption. The absorption corresponding to the transition between the states ground state and 2nd excited state is 433.5 which corresponding to blue shift transition. The highest wavelength absorption was at 389.3 nm wavelength. States 1st and 2nd corresponding to the visible spectrum and the remaining all other transition corresponding to the UV range. In presence of water, the relative energies of all six doublet states and transition dipole moments are listed in table 2

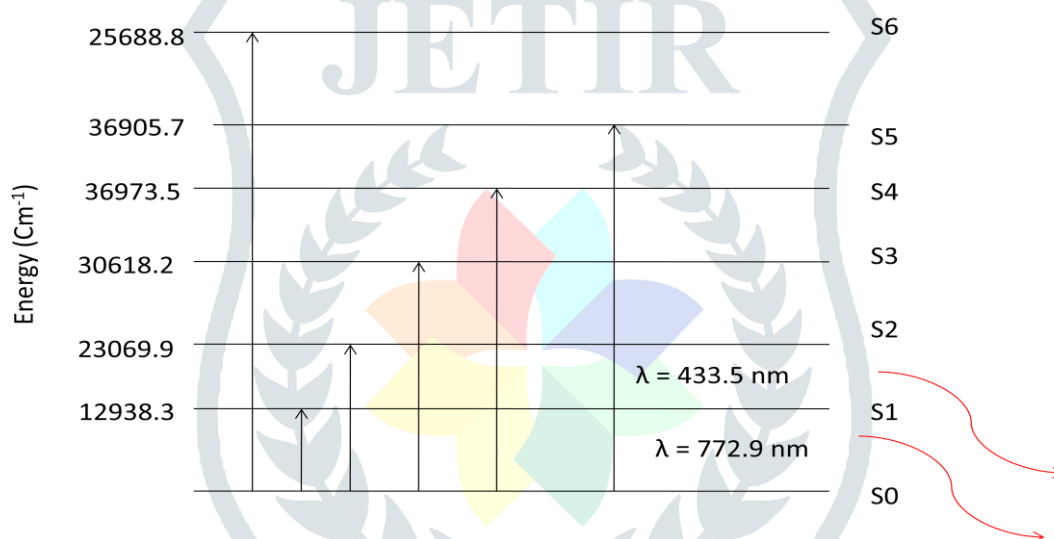


Fig.2 CASSCF/ NEVPT2 spectrum of six electronically excited states of bacteriorhodopsin connected with lysine amino acid.

Circular dichroism spectra and UV spectra

The circular dichroism is property possessed by some absorbing light material to different extents and depends upon the polarization of incident beam. The difference of right circularly polarized light and left circularly polarized light was observed in terms of circular dichroism spectra. The material said to exhibit circular dichroism spectra. The CD spectra are very important for study of peptide bonds in proteins and its contribution is invaluable as comparison to x-ray crystallography. Structural damage is recorded by CD spectra under UV exposure to retinal-lysine combination. Any structural and environmental change to protein will affect the CD spectrum. The computed CD-UV spectra of retinal-lysine molecule of bR is shown in figure 3 and absorption spectra is shown in figure 4. It has been seen that absorption below the 238.1 nm or 5.9 eV is the absorption due to peptide bond with lysine amino acid which is connected with retinal chromophore. The transition states ($n \rightarrow \pi^*$) was occurred below the 5.9 eV energy of the UV photons. The most intense transition found to occur at energy 5.3 eV of UV photons. This transition was corresponding to $\pi \rightarrow \pi^*$ states orbitals transition which is not polarized along the any specific bond. The intensity of transition depends on F and W torsion angle [54]. The CD spectra is results of alpha-helix, beta-sheet and random coil structure in proteins [55, 56]. CD spectra were revealing a secondary structure in proteins. The negative peaks were found between energy range 4.4 eV to 5.5 eV for secondary structure of lysine amino acid. The nearly occurred peaks were found because of doublet spin coupling factor. Positive peaks were shifted along the longer wavelength absorption. The peaks near 4.4 eV and 5.7 eV in free space were known as conservative couplets. These couplets indication were the sign of removal of methyl group from the asymmetric carbon atom in UV region. There were two positive couplet peaks were found near 5.9 eV and 6.5 eV UV- CD spectrum. Highest peaks at positive side were found near to PSB linkage which is more interactive with photon for charge transfers states. The photo isomerization has been shown along the PSB association [46].

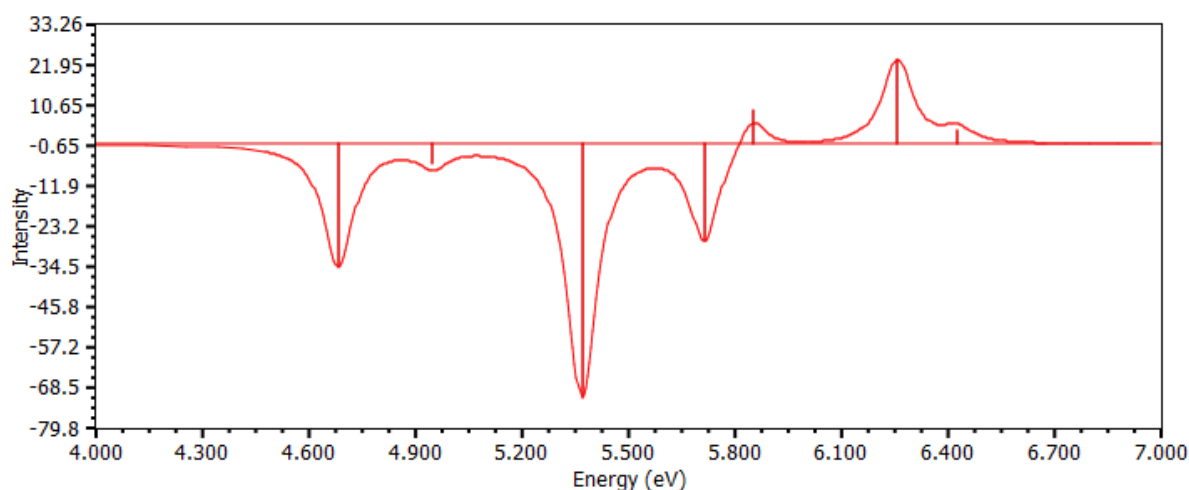


Fig.3 UV-CD spectra of retinal chromophore bR protein with TD-DFT method in free space

All proton drive by photon pump mechanism in bR was control along the protonated Schiff base. It has been observed by CD spectroscopy about the structural change in bR protein. We have studied the retinal chromophore in presence of water. The dielectric constant of water is 80.8 and its refractive index is 1.33. To study the solvent effect, we have used the cosmo method for calculation of excited states energies in presence of water by ORCA. The CD spectra and UV absorption spectra were calculated in presence of water.

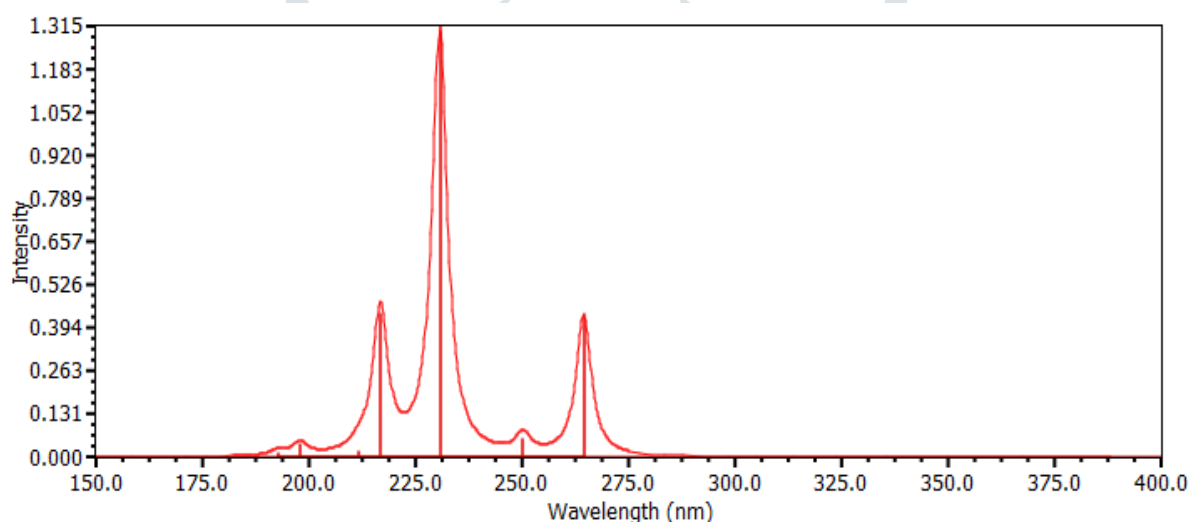


Fig.4 UV Absorption spectra of bacteriorhodopsin chromophore with TD-DFT in free space

The computed CD-UV spectra of retinal-lysine of bR is shown in figure 5 and UV absorption the absorption spectra is shown in figure 6. In presence of water, highest the spectral peak were observed around 231 nm in free space which shift to higher wavelength and the value of the peak is 238 nm. All peaks in presence of water were shifted to higher wavelength and intensity of absorption spectra was decreasing. All spectrum were around to all $n \rightarrow \pi^*$, $\pi \rightarrow \pi^*$ and $n \rightarrow \pi$ doublets states transition. Spectral peaks will shifts to higher wavelength because of change of dielectric constant. The change of medium changes the structural parameter of the molecule. Retinal chromophore is an optical active molecule in presence of water as its polarization states changes with change of medium. The dielectric medium a (bR) acts as tuner. We have seen spectral tuning clearly for bR. The spectral tuning is evident from figure 3, 4, 5 and 6.

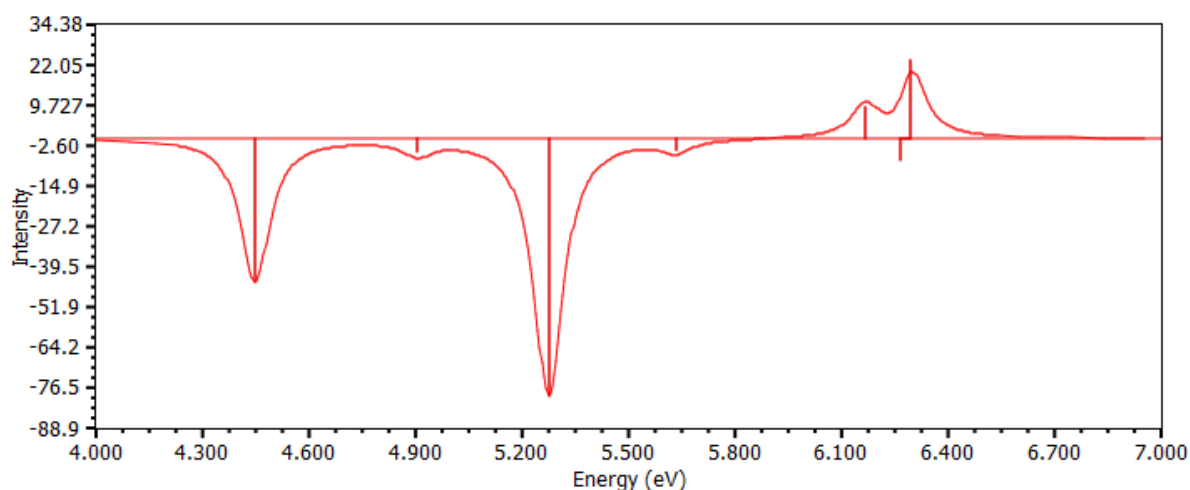


Fig.5 UV- CD of retinal chromophore spectra of bR protein with TD-DFT method in presence of water

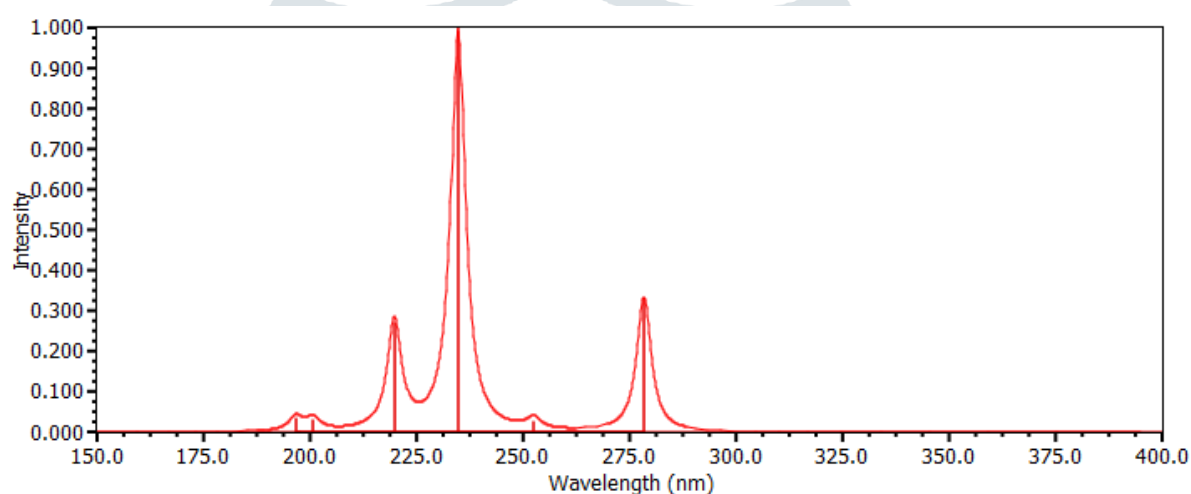


Fig.6 UV Absorption spectra of bacteriorhodopsin chromophore with TD-DFT method in water space

Conclusions

The good agreement among our theoretical results and available experimental results shows that modern quantum mechanical method can not only reproduce but also interpret spectral properties of the bacteriorhodopsin protein. Our approach of combining very efficient (NEVPT2/ CASSCF) and very accurate MP2 / (TD-DFT methods allows a comprehensive, qualitative investigation of the spectral shift including the analysis of dynamical effects.

The mechanisms underlying spectral tuning in retinal protein have been computationally examined highly homologous retinal bR. The spectral tuning between S0-S1 is 772.9 nm and between S0-S2 434 nm was found in free space. These spectral tuning was found in presence water are 774.1 nm in between states (S0-S1) and 439.5 nm in between states (S0-S2). The transition between ground state and second excited state was nearly similar to the experimental results performed in so many research articles available in literature.

The analysis of calculated energy shows that difference between ground state and first excited is mainly because of electronic reorganization in retinal and some residue of amino acid are not included in calculations. The successful explanation of bR spectral shift gives new path for investigation biological molecules on the basis of ab initio quantum chemical calculation for spectral tuning in visual pigments. It can be applied to explain the optical properties of mutant rhodopsin which displays blue or red shifted to those of wild type.

References

1. Spudich, J.L., et al., *Retinylidene Proteins: Structures and Functions from Archaea to Humans*. Annual Review of Cell and Developmental Biology, 2000. **16**(1): p. 365-392.
2. van der Horst, M.A. and K.J. Hellminger, *Photoreceptor Proteins, "Star Actors of Modern Times": A Review of the Functional Dynamics in the Structure of Representative Members of Six Different Photoreceptor Families*. Accounts of Chemical Research, 2004. **37**(1): p. 13-20.
3. Nakanishi, K. and R. Crouch, *Application of Artificial Pigments to Structure Determination and Study of Photoinduced Transformations of Retinal Proteins*. Israel Journal of Chemistry, 1995. **35**(3-4): p. 253-272.

4. Kleinschmidt, J. and F.I. Harosi, *Anion sensitivity and spectral tuning of cone visual pigments in situ*. Proceedings of the National Academy of Sciences, 1992. **89**(19): p. 9181.
5. Demoulin, B., et al., *Fine Tuning of Retinal Photoinduced Decay in Solution*. The Journal of Physical Chemistry Letters, 2017. **8**(18): p. 4407-4412.
6. Li, Y.-T., et al., *A Review on Bacteriorhodopsin-Based Bioelectronic Devices*. Sensors (Basel, Switzerland), 2018. **18**(5): p. 1368.
7. Ebrey, T. and Y. Koutalos, *Vertebrate Photoreceptors*. Progress in Retinal and Eye Research, 2001. **20**(1): p. 49-94.
8. Belrhali, H., et al., *Protein, lipid and water organization in bacteriorhodopsin crystals: a molecular view of the purple membrane at 1.9 Å resolution*. Structure, 1999. **7**(8): p. 909-917.
9. Essen, L.O., et al., *Lipid patches in membrane protein oligomers: Crystal structure of the bacteriorhodopsin-lipid complex*. Proceedings of the National Academy of Sciences, 1998. **95**(20): p. 11673.
10. Pebay-Peyroula, E., et al., *X-ray Structure of Bacteriorhodopsin at 2.5 Angstroms from Microcrystals Grown in Lipidic Cubic Phases*. Science, 1997. **277**(5332): p. 1676.
11. Irving, C.S., G.W. Byers, and P.A. Leermakers, *Spectroscopic model for the visual pigments. Influence of microenvironmental polarizability*. Biochemistry, 1970. **9**(4): p. 858-864.
12. Blatz, P.E. and P.A. Liebman, *Wavelength regulation in visual pigments*. Experimental Eye Research, 1973. **17**(6): p. 573-580.
13. Honig, B., et al., *An external point-charge model for wavelength regulation in visual pigments*. Journal of the American Chemical Society, 1979. **101**(23): p. 7084-7086.
14. Schulten, K., U. Dinur, and B. Honig, *The spectra of carbonium ions, cyanine dyes, and protonated Schiff base polyenes*. The Journal of Chemical Physics, 1980. **73**(8): p. 3927-3935.
15. Bèjà, O., et al., *Proteorhodopsin phototrophy in the ocean*. Nature, 2001. **411**: p. 786.
16. Rattner, A., H. Sun, and J. Nathans, *Molecular Genetics of Human Retinal Disease*. Annual Review of Genetics, 1999. **33**(1): p. 89-131.
17. Nathans, J., *In the eye of the beholder: Visual pigments and inherited variation in human vision*. Cell, 1994. **78**(3): p. 357-360.
18. Chang, C.H., et al., *REGENERATION OF BLUE AND PURPLE MEMBRANES FROM DEIONIZED BLEACHED MEMBRANES OF Halobacterium halobium*. Photochemistry and Photobiology, 1988. **47**(2): p. 261-265.
19. Lanyi, J.K., *Molecular Mechanism of Ion Transport in Bacteriorhodopsin: Insights from Crystallographic, Spectroscopic, Kinetic, and Mutational Studies*. The Journal of Physical Chemistry B, 2000. **104**(48): p. 11441-11448.
20. Haupts, U., et al., *General Concept for Ion Translocation by Halobacterial Retinal Proteins: The Isomerization/Switch/Transfer (IST) Model*. Biochemistry, 1997. **36**(1): p. 2-7.
21. Hoff, W.D., K.-H. Jung, and J.L. Spudich, *MOLECULAR MECHANISM OF PHOTOSIGNALING BY ARCHAEAL SENSORY RHODOPSINS*. Annual Review of Biophysics and Biomolecular Structure, 1997. **26**(1): p. 223-258.
22. Luzhkov, V. and A. Warshel, *Microscopic calculations of solvent effects on absorption spectra of conjugated molecules*. Journal of the American Chemical Society, 1991. **113**(12): p. 4491-4499.
23. Mathies, R. and L. Stryer, *Retinal has a highly dipolar vertically excited singlet state: implications for vision*. Proceedings of the National Academy of Sciences of the United States of America, 1976. **73**(7): p. 2169-2173.
24. Warshel, A. and Z.T. Chu, *Nature of the Surface Crossing Process in Bacteriorhodopsin: Computer Simulations of the Quantum Dynamics of the Primary Photochemical Event*. The Journal of Physical Chemistry B, 2001. **105**(40): p. 9857-9871.
25. Houjou, H., Y. Inoue, and M. Sakurai, *Study of the Opsin Shift of Bacteriorhodopsin: Insight from QM/MM Calculations with Electronic Polarization Effects of the Protein Environment*. The Journal of Physical Chemistry B, 2001. **105**(4): p. 867-879.
26. Sakurai, M., et al., *Decisive Role of Electronic Polarization of the Protein Environment in Determining the Absorption Maximum of Halorhodopsin*. Journal of the American Chemical Society, 2003. **125**(10): p. 3108-3112.
27. Warshel, A., *Calculations of chemical processes in solutions*. The Journal of Physical Chemistry, 1979. **83**(12): p. 1640-1652.

28. Houjou, H., Y. Inoue, and M. Sakurai, *Physical Origin of the Opsin Shift of Bacteriorhodopsin. Comprehensive Analysis Based on Medium Effect Theory of Absorption Spectra*. Journal of the American Chemical Society, 1998. **120**(18): p. 4459-4470.
29. Albeck, A., et al., *Carbon-13 NMR studies of model compounds for bacteriorhodopsin: factors affecting the retinal chromophore chemical shifts and absorption maximum*. Journal of the American Chemical Society, 1992. **114**(7): p. 2400-2411.
30. Dimitrov, D., et al., *Engineering and Characterization of an Enhanced Fluorescent Protein Voltage Sensor*. PLOS ONE, 2007. **2**(5): p. e440.
31. Bates, M., B. Huang, and X. Zhuang, *Super-resolution microscopy by nanoscale localization of photo-switchable fluorescent probes*. Current Opinion in Chemical Biology, 2008. **12**(5): p. 505-514.
32. Day, R.N. and M.W. Davidson, *The fluorescent protein palette: tools for cellular imaging*. Chemical Society Reviews, 2009. **38**(10): p. 2887-2921.
33. Meyer, A.J. and T.P. Dick, *Fluorescent Protein-Based Redox Probes*. Antioxidants & Redox Signaling, 2010. **13**(5): p. 621-650.
34. Narita, A., et al., *Visible sensing of nucleic acid sequences using a genetically encodable unmodified mRNA probe*. Nucleic Acids Symposium Series, 2006. **50**(1): p. 283-284.
35. Newman, R.H., M.D. Fosbrink, and J. Zhang, *Genetically Encodable Fluorescent Biosensors for Tracking Signaling Dynamics in Living Cells*. Chemical Reviews, 2011. **111**(5): p. 3614-3666.
36. Schifferer, M. and O. Griesbeck, *Application of aptamers and autofluorescent proteins for RNA visualization*. Integrative Biology, 2009. **1**(8-9): p. 499-505.
37. Shank, N.I., et al., *Enhanced Photostability of Genetically Encodable Fluoromodules Based on Fluorogenic Cyanine Dyes and a Promiscuous Protein Partner*. Journal of the American Chemical Society, 2009. **131**(36): p. 12960-12969.
38. Berthold, P., et al., *Channelrhodopsin-1 Initiates Phototaxis and Photophobic Responses in <i>Chlamydomonas</i> by Immediate Light-Induced Depolarization*. The Plant Cell, 2008. **20**(6): p. 1665.
39. Kianianmomeni, A., et al., *Channelrhodopsins of <i>Volvox carteri</i> Are Photochromic Proteins That Are Specifically Expressed in Somatic Cells under Control of Light, Temperature, and the Sex Inducer*. Plant Physiology, 2009. **151**(1): p. 347.
40. Paternolli, C., et al., *Photoreversibility and photostability in films of octopus rhodopsin isolated from octopus photoreceptor membranes*. Journal of Biomedical Materials Research Part A, 2008. **88A**(4): p. 947-951.
41. Kawanabe, A., et al., *Photochromism of Anabaena Sensory Rhodopsin*. Journal of the American Chemical Society, 2007. **129**(27): p. 8644-8649.
42. Strambi, A., et al., *<i>Anabaena</i> sensory rhodopsin is a light-driven unidirectional rotor*. Proceedings of the National Academy of Sciences, 2010. **107**(50): p. 21322.
43. Kralj, J.M., et al., *Electrical Spiking in <i>Escherichia coli</i> Probed with a Fluorescent Voltage-Indicating Protein*. Science, 2011. **333**(6040): p. 345.
44. Kralj, J.M., et al., *Optical recording of action potentials in mammalian neurons using a microbial rhodopsin*. Nature Methods, 2011. **9**: p. 90.
45. Roos, B.O., *Theoretical Studies of Electronically Excited States of Molecular Systems Using Multiconfigurational Perturbation Theory*. Accounts of Chemical Research, 1999. **32**(2): p. 137-144.
46. Fantacci, S., A. Migani, and M. Olivucci, *CASPT2//CASSCF and TDDFT//CASSCF Mapping of the Excited State Isomerization Path of a Minimal Model of the Retinal Chromophore*. The Journal of Physical Chemistry A, 2004. **108**(7): p. 1208-1213.
47. Barone, V., et al., *Electron Transfer in the [Pt(NH₃)₄]²⁺ [W(CN)₈]³⁻ Donor-Acceptor System. The Environment Effect: A Time-Dependent Density Functional Study*. Journal of the American Chemical Society, 2001. **123**(43): p. 10742-10743.
48. Collins, C.L., K.G. Dyall, and H.F. Schaefer III, *Relativistic and correlation effects in CuH, AgH, and AuH: Comparison of various relativistic methods*. The Journal of chemical physics, 1995. **102**(5): p. 2024-2031.
49. Luecke, H., et al., *Structural Changes in Bacteriorhodopsin During Ion Transport at 2 Angstrom Resolution*. Science, 1999. **286**(5438): p. 255.
50. Neese, F., *The ORCA program system*. Wiley Interdisciplinary Reviews: Computational Molecular Science, 2011. **2**(1): p. 73-78.

51. Kalatzis, F.G. and I.N. Demetropoulos, *A BSSE-corrected CASSCF/NEVPT2 procedure. An application to weakly bonded OH.. π heterodimer complexes*. Molecular Physics, 2007. **105**(17-18): p. 2335-2343.
52. Hayashi, S., et al., *Structural Determinants of Spectral Tuning in Retinal Proteins Bacteriorhodopsin vs Sensory Rhodopsin II*. The Journal of Physical Chemistry B, 2001. **105**(41): p. 10124-10131.
53. Chizhov, I., et al., *The Photophobic Receptor from Natronobacterium pharaonis: Temperature and pH Dependencies of the Photocycle of Sensory Rhodopsin II*. Biophysical Journal, 1998. **75**(2): p. 999-1009.
54. Hong, M., *Determination of Multiple φ -Torsion Angles in Proteins by Selective and Extensive ^{13}C Labeling and Two-Dimensional Solid-State NMR*. Journal of Magnetic Resonance, 1999. **139**(2): p. 389-401.
55. Berova N., N.K., Woody R.W., *Circular Dichroism: Principles and Applications*, 2nd edn. 2000, New York, USA: Wiley-VCH.
56. G.G., H., *Spectroscopy for the Biological Sciences*. 2005, USA, New York: John Wiley & Sons,.

